

Decoupling the coupled DGLAP evolution equations: an analytic solution to pQCD

Martin M. Block

Department of Physics and Astronomy, Northwestern University, Evanston, IL 60208

Loyal Durand

Department of Physics, University of Wisconsin, Madison, WI 53706

Phuoc Ha

Department of Physics, Astronomy and Geosciences, Towson University, Towson, MD 21252

Douglas W. McKay

Department of Physics and Astronomy, University of Kansas, Lawrence, KS 66045

(Dated: April 12, 2010)

Using Laplace transform techniques, along with newly-developed accurate numerical inverse Laplace transform algorithms [1, 2], we *decouple* the solutions for the singlet structure function $F_s(x, Q^2)$ and $G(x, Q^2)$ of the two leading-order coupled singlet DGLAP equations, allowing us to write fully decoupled solutions:

$$\begin{aligned} F_s(x, Q^2) &= \mathcal{F}_s(F_{s0}(x), G_0(x)), \\ G(x, Q^2) &= \mathcal{G}(F_{s0}(x), G_0(x)). \end{aligned}$$

Here \mathcal{F}_s and \mathcal{G} are known functions—found using the DGLAP splitting functions—of the functions $F_{s0}(x) \equiv F_s(x, Q_0^2)$ and $G_0(x) \equiv G(x, Q_0^2)$, the chosen starting functions at the virtuality Q_0^2 . As a proof of method, we compare our numerical results from the above equations with the published MSTW LO gluon and singlet F_s distributions [3], starting from their initial values at $Q_0^2 = 1 \text{ GeV}^2$. Our method completely decouples the two LO distributions, at the same time guaranteeing that both distributions satisfy the singlet coupled DGLAP equations. It furnishes us with a new tool for readily obtaining the effects of the starting functions (independently) on the gluon and singlet structure functions, as functions of both Q^2 and Q_0^2 . In addition, it can also be used for non-singlet distributions, thus allowing one to solve analytically for individual quark and gluon distributions values at a given x and Q^2 , with typical numerical accuracies of about 1 part in 10^5 , rather than having to evolve numerically coupled integral-differential equations on a two-dimensional grid in x, Q^2 , as is currently done.

Accurate knowledge of gluon distribution functions at small Bjorken x and large virtuality Q^2 plays a vital role in estimating QCD backgrounds and in calculating gluon-initiated processes, and thus in our ability to search for new physics at the Large Hadron Collider.

The gluon and quark distribution functions have traditionally been determined simultaneously by fitting experimental data on neutral- and charged-current deep inelastic scattering processes and some jet data over a large domain of values of x and Q^2 . The distributions at small x and large Q^2 are determined mainly by the proton structure function $F_2^{\gamma^*p}(x, Q^2)$ measured in deep inelastic ep (or γ^*p) scattering. The fitting process starts with an initial Q_0^2 , typically less than the square of the c quark mass, $m_c^2 \approx 2 \text{ GeV}^2$, and individual quark and gluon trial distributions parameterized with pre-determined shapes, given as functions of x for the chosen Q_0^2 . The distributions are then evolved numerically on a two-dimensional grid in x and Q^2 to larger Q^2 using the coupled integral-differential DGLAP equations [4–6], typically in leading order (LO) and next-to-leading order (NLO), and the results used to predict the measured quantities. The final distributions are then determined by adjusting the input parameters to obtain a best fit to the data. This procedure is very indirect in the case of the gluon: the gluon distribution $G(x, Q^2) = xg(x, Q^2)$ does not contribute directly to the accurately determined structure function $F_2^{\gamma^*p}(x, Q^2)$, and is determined only through the quark distributions in conjunction with the evolution equations, or at large x , from jet data. For recent determinations of the gluon and quark distributions, see [3, 7–10].

In the following, we will summarize our analytic method for determining the singlet structure functions $F_s(x, Q^2)$ and $G(x, Q^2)$ *directly* and *individually*, using as input $F_{s0}(x) \equiv F_s(x, Q_0^2)$ and $G_0(x) \equiv G(x, Q_0^2)$, where Q_0^2 is arbitrary, with the guarantee that each individually satisfies the coupled DGLAP equations. The method can be extended simply to embrace non-singlet functions, so that it can be used to find individual quark distributions. However, we will not pursue that goal in this communication. Instead, we give a numerical demonstration by using the LO MSTW [3] F_{s0} and G_0 at $Q_0^2 = 1 \text{ GeV}^2$ to generate their singlet structure functions and gluon distributions at large Q^2 . Because our basic solutions are analytic, we readily obtain numerical accuracies for $F_s(x, Q^2)$ and $G(x, Q^2)$ of better than 1 part in 10^5 for all Bjorken- x and virtuality Q^2 considered.

Our approach uses a somewhat unusual application of Laplace transforms [11, 12], in which we first introduce the variable $v \equiv \ln(1/x)$ into the coupled DGLAP equations, then Laplace transform these coupled integral-differential equations in v space to obtain coupled homogeneous first-order differential equations in the variable Q^2 . The parameters of these transformed equations are known functions of s , the Laplace-space variable. These equations are then solved analytically. Finally, using fast and accurate numerical inverse Laplace transform algorithms [1, 2], we transform the solutions back into v space, and, finally, into Bjorken x -space, i.e., $F_s(x, Q^2) = \mathcal{F}_s(F_{s0}(x), G_0(x))$ and $G(x, Q^2) = \mathcal{G}(F_{s0}(x), G_0(x))$, where the functions \mathcal{F} and \mathcal{G} are determined by the splitting functions in the DGLAP equations.

Our method can be generalized to NLO, but for brevity, we will limit ourselves to LO in this paper. We write the coupled LO DGLAP equations [11, 12] as

$$\begin{aligned} \frac{4\pi}{\alpha_s(Q^2)} \frac{\partial F_s}{\partial \ln Q^2}(x, Q^2) &= 4F_s(x, Q^2) + \frac{16}{3}F_s(x, Q^2) \ln \frac{1-x}{x} + \frac{16}{3}x \int_x^1 \left(\frac{F_s(z, Q^2)}{z} - \frac{F_s(x, Q^2)}{x} \right) \frac{dz}{z-x} \\ &\quad - \frac{8}{3}x \int_x^1 F_s(z, Q^2) \left(1 + \frac{x}{z} \right) \frac{dz}{z^2} + 2n_f x \int_x^1 G(z, Q^2) \left(1 - 2\frac{x}{z} + 2\frac{x^2}{z^2} \right) \frac{dz}{z^2}, \end{aligned} \quad (1)$$

$$\begin{aligned} \frac{4\pi}{\alpha_s(Q^2)} \frac{\partial G}{\partial \ln Q^2}(x, Q^2) &= \frac{33-2n_f}{3}G(x, Q^2) + 12G(x, Q^2) \ln \frac{1-x}{x} + 12x \int_x^1 \left(\frac{G(z, Q^2)}{z} - \frac{G(x, Q^2)}{x} \right) \frac{dz}{z-x} \\ &\quad + 12x \int_x^1 G(z, Q^2) \left(\frac{z}{x} - 2 + \frac{x}{z} - \frac{x^2}{z^2} \right) \frac{dz}{z^2} + \frac{8}{3} \int_x^1 F_s(z, Q^2) \left(1 + \left(1 - \frac{x}{z} \right)^2 \right) \frac{dz}{z}. \end{aligned} \quad (2)$$

Here $\alpha_s(Q^2)$ is the running strong coupling constant, given in LO by

$$\alpha_s(Q^2) = \frac{4\pi}{(11 - \frac{2}{3}n_f) \ln(Q^2/\Lambda_{n_f}^2)}, \quad (3)$$

where Λ_{n_f} is fixed so that Λ_5 reproduces $\alpha_s(M_Z^2)$, and the other Λ 's (Λ_4 and Λ_3) are adjusted so that α_s is continuous across the boundaries $Q^2 = M_b^2$ and M_c^2 , respectively, where M_b and M_c are the masses of the b and c quarks.

We now examine the last two terms of line 1 in Eq. (1) and rewrite them, introducing the variable changes $v = \ln(1/x)$, $w = \ln(1/z)$, and the notation $\hat{F}_s(v, Q^2) \equiv F_s(e^{-v}, Q^2)$, $\hat{G}(v, Q^2) \equiv G(e^{-v}, Q^2)$ as

$$\begin{aligned} &\frac{16}{3}\hat{F}_s(v, Q^2) \ln(e^v - 1) + \frac{16}{3} \int_0^v \left(\hat{F}_s(w, Q^2) - \hat{F}_s(v, Q^2)e^{v-w} \right) \frac{1}{e^{v-w} - 1} dw \\ &= \frac{16}{3} \int_0^v \frac{\partial \hat{F}_s}{\partial w}(w, Q^2) \ln \left(1 - e^{-(v-w)} \right) dw. \end{aligned} \quad (4)$$

where the final result—the last line in Eq. (4)—is found by replacing the upper limit v in integral of line 1 of Eq. (4) by $v - \epsilon$, carrying out the integrals, doing a partial integration and then taking the limit as $\epsilon \rightarrow 0$. Similarly, we find for the last two terms of line 1 in Eq. (2), that

$$\begin{aligned} &12\hat{G}(v, Q^2) \ln(e^v - 1) + 12 \int_0^v \left(\hat{G}(w, Q^2) - \hat{G}(v, Q^2)e^{v-w} \right) \frac{1}{e^{v-w} - 1} dw \\ &= 12 \int_0^v \frac{\partial \hat{G}}{\partial w}(w, Q^2) \ln \left(1 - e^{-(v-w)} \right) dw. \end{aligned} \quad (5)$$

We next rewrite Eq. (1) and Eq. (2), in terms of the new variable v , as

$$\begin{aligned} \frac{4\pi}{\alpha_s(Q^2)} \frac{\partial \hat{F}_s}{\partial \ln Q^2}(v, Q^2) &= 4\hat{F}_s(v, Q^2) + \frac{16}{3} \int_0^v \frac{\partial \hat{F}_s}{\partial w}(w, Q^2) \ln(1 - e^{w-v}) dw \\ &\quad - \frac{8}{3} \int_0^v \hat{F}_s(w, Q^2) \left(e^{-(v-w)} + e^{-2(v-w)} \right) dw \\ &\quad + 2n_f \int_0^v \hat{G}(w, Q^2) \left(e^{-(v-w)} - 2e^{-2(v-w)} + 2e^{-3(v-w)} \right) dw, \end{aligned} \quad (6)$$

$$\begin{aligned} \frac{4\pi}{\alpha_s(Q^2)} \frac{\partial \hat{G}}{\partial \ln Q^2}(v, Q^2) &= \frac{33 - 2n_f}{3} \hat{G}(v, Q^2) + 12 \int_0^v \frac{\partial \hat{G}}{\partial w}(w, Q^2) \ln(1 - e^{-(v-w)}) dw \\ &\quad + 12 \int_0^v \hat{G}(w, Q^2) \left(1 - 2e^{-(v-w)} + e^{-2(v-w)} - e^{-3(v-w)} \right) dw \\ &\quad + \frac{8}{3} \int_0^v \hat{F}_s(w, Q^2) \left(1 + \left(1 - e^{-(v-w)} \right)^2 \right) dw. \end{aligned} \quad (7)$$

All of the integrals in Eq. (6) and Eq. (7) are convolutions. Introducing Laplace transforms allows us to factor these integrals, since the Laplace transform of a convolution is the product of the Laplace transform of the factors, i.e.,

$$\mathcal{L} \left[\int_0^v F[w] H[v-w] dw; s \right] = \mathcal{L}[F[v]; s] \times \mathcal{L}[H[v]; s]. \quad (8)$$

Defining the Laplace transforms

$$f(s, Q^2) \equiv \mathcal{L} \left[\hat{F}_s(v, Q^2); s \right], \quad g(s, Q^2) \equiv \mathcal{L} [\hat{G}(v, Q^2); s] \quad (9)$$

and noting that

$$\mathcal{L} \left[\frac{\partial \hat{F}_s}{\partial w}(w, Q^2); s \right] = sf(s, Q^2), \quad \mathcal{L} \left[\frac{\partial \hat{G}}{\partial w}(w, Q^2); s \right] = sg(s, Q^2), \quad (10)$$

we can factor the Laplace transforms of Eq. (6) and Eq. (7) into two coupled ordinary first order differential equations in Laplace space s with Q^2 -dependent coefficients. These can be written as

$$\frac{\partial f}{\partial \ln Q^2}(s, Q^2) = \frac{\alpha_s(Q^2)}{4\pi} \Phi_f(s) f(s, Q^2) + \frac{\alpha_s(Q^2)}{4\pi} \Theta_f(s) g(s, Q^2), \quad (11)$$

$$\frac{\partial g}{\partial \ln Q^2}(s, Q^2) = \frac{\alpha_s(Q^2)}{4\pi} \Phi_g(s) g(s, Q^2) + \frac{\alpha_s(Q^2)}{4\pi} \Theta_g(s) f(s, Q^2), \quad (12)$$

whose coefficients Φ and Θ are given by

$$\Phi_f(s) = 4 - \frac{8}{3} \left(\frac{1}{s+1} + \frac{1}{s+2} + 2(\psi(s+1) + \gamma_E) \right) \quad (13)$$

$$\Theta_f(s) = 2n_f \left(\frac{1}{s+1} - \frac{2}{s+2} + \frac{2}{s+3} \right), \quad (14)$$

$$\Phi_g(s) = \frac{33 - 2n_f}{3} + 12 \left(\frac{1}{s} - \frac{2}{s+1} + \frac{1}{s+2} - \frac{1}{s+3} - \psi(s+1) - \gamma_E \right) \quad (15)$$

$$\Theta_g(s) = \frac{8}{3} \left(\frac{2}{s} - \frac{2}{s+1} + \frac{1}{s+2} \right), \quad (16)$$

where $\psi(x)$ is the digamma function and $\gamma_E = 0.5772156 \dots$ is Euler's constant.

The solution of the coupled equations in Eq. (11) and Eq. (12) in terms of initial values of the functions f and g , specified as functions of s at virtuality Q_0^2 , is straightforward. The Q^2 dependence of the solutions is expressed entirely through the function

$$\tau(Q^2, Q_0^2) = \frac{1}{4\pi} \int_{Q_0^2}^{Q^2} \alpha_s(Q'^2) d \ln Q'^2. \quad (17)$$

With the initial conditions $f_0(s) \equiv f(s, Q_0^2)$ and $g_0(s) \equiv g(s, Q_0^2)$, the solutions are

$$f(s, \tau) = k_{ff}(s, \tau)f_0(s) + k_{fg}(s, \tau)g_0(s), \quad (18)$$

$$g(s, \tau) = k_{gg}(s, \tau)g_0(s) + k_{gf}(s, \tau)f_0(s), \quad (19)$$

where the coefficient functions in the solution are

$$k_{ff}(s, \tau) \equiv e^{\frac{\tau}{2}(\Phi_f(s) + \Phi_g(s))} \left[\cosh\left(\frac{\tau}{2}R(s)\right) + \frac{\sinh\left(\frac{\tau}{2}R(s)\right)}{R(s)} (\Phi_f(s) - \Phi_g(s)) \right], \quad (20)$$

$$k_{fg}(s, \tau) \equiv \left(e^{\frac{\tau}{2}(\Phi_f(s) + \Phi_g(s) + R(s))} - e^{\frac{\tau}{2}(\Phi_f(s) + \Phi_g(s) - R(s))} \right) \frac{\Theta_f(s)}{R(s)}, \quad (21)$$

$$k_{gg}(s, \tau) \equiv e^{\frac{\tau}{2}(\Phi_f(s) + \Phi_g(s))} \left[\cosh\left(\frac{\tau}{2}R(s)\right) - \frac{\sinh\left(\frac{\tau}{2}R(s)\right)}{R(s)} (\Phi_f(s) - \Phi_g(s)) \right], \quad (22)$$

$$k_{gf}(s, \tau) \equiv \left(e^{\frac{\tau}{2}(\Phi_f(s) + \Phi_g(s) + R(s))} - e^{\frac{\tau}{2}(\Phi_f(s) + \Phi_g(s) - R(s))} \right) \frac{\Theta_g(s)}{R(s)}, \quad (23)$$

with $R(s) \equiv \sqrt{(\Phi_f(s) - \Phi_g(s))^2 + 4\Theta_f(s)\Theta_g(s)}$.

Let us now define four kernels K_{FF} , K_{FG} , K_{GF} and K_{GG} , the inverse Laplace transforms of the $k's$, i.e.,

$$K_{FF}(v, \tau) \equiv \mathcal{L}^{-1}[k_{ff}(s, \tau); v], \quad K_{FG}(v, \tau) \equiv \mathcal{L}^{-1}[k_{fg}(s, \tau); v], \quad (24)$$

$$K_{GG}(v, \tau) \equiv \mathcal{L}^{-1}[k_{gg}(s, \tau); v], \quad K_{GF}(v, \tau) \equiv \mathcal{L}^{-1}[k_{gf}(s, \tau); v]. \quad (25)$$

It is evident from Eqs. (17), (21), and (23) that K_{FG} and K_{GF} vanish for $Q^2 = Q_0^2$ where $\tau(Q^2, Q_0^2) = 0$. It can also be shown without difficulty that for $\tau = 0$, $K_{FF}(v, 0) = K_{GG}(v, 0) = \delta(v)$.

The initial boundary conditions at Q_0^2 are given by $F_{s0}(x) = F_s(x, Q_0^2)$ and $G_0(x) = G(x, Q_0^2)$. In v -space, $\hat{F}_{s0}(v) \equiv F_{s0}(e^{-v})$ and $\hat{G}_0(v) \equiv G_0(e^{-v})$ are the inverse Laplace transforms of $f_0(s)$ and $g_0(s)$, respectively, i.e.,

$$\hat{F}_{s0}(v) \equiv \mathcal{L}^{-1}[f_0(s); v] \text{ and } \hat{G}_0(v) \equiv \mathcal{L}^{-1}[g_0(s); v]. \quad (26)$$

Finally, we can write our *decoupled* solutions in v -space in terms of the convolution integrals

$$\hat{F}_s(v, Q^2) = \int_0^v K_{FF}(v-w, \tau(Q^2, Q_0^2)) \hat{F}_{s0}(w) dw + \int_0^v K_{FG}(v-w, \tau(Q^2, Q_0^2)) \hat{G}_0(w) dw, \quad (27)$$

$$\hat{G}(v, Q^2) = \int_0^v K_{GG}(v-w, \tau(Q^2, Q_0^2)) \hat{G}_0(w) dw + \int_0^v K_{GF}(v-w, \tau(Q^2, Q_0^2)) \hat{F}_{s0}(w) dw. \quad (28)$$

Noting again that $v \equiv \ln(1/x)$, in the usual variables—Bjorken- x and virtuality Q^2 —we readily find the desired *decoupled* $F_s(x, Q^2)$ and $G(x, Q^2)$ from the above decoupled solutions for $\hat{F}_s(v, Q^2)$ and $\hat{G}(v, Q^2)$, requiring only a knowledge of the initial values $F_{s0}(x)$ and $G_0(x)$ at Q_0^2 .

For *non-singlet* distributions $F_{ns}(x, Q^2)$, such as the difference between the u and d quark distributions, $x[u(x, Q^2) - d(x, Q^2)]$, we can schematically write the logarithmic derivative of F_{ns} as the convolution of $F_{ns}(x, Q^2)$ with the non-singlet splitting function $\mathcal{K}_{ns}(x)$ (using the convolution symbol \otimes), i.e.,

$$\frac{4\pi}{\alpha_s(Q^2)} \frac{\partial F_{ns}}{\partial \ln(Q^2)}(x, Q^2) = F_{ns} \otimes \mathcal{K}_{ns}. \quad (29)$$

After changing to the variable $v = \ln(1/x)$ and going to Laplace space s , we find the simple solution

$$f_{ns}(s, \tau) = e^{\tau\Phi_{ns}(s)} f_{ns0}(s), \quad \text{where } \Phi_{ns}(s) = \mathcal{L} \left[e^{-v} \hat{\mathcal{K}}_{ns}(v); s \right] \quad \text{and } \hat{\mathcal{K}}_{ns}(v) = \mathcal{K}_{ns}(e^{-v}). \quad (30)$$

Thus we can find *any* non-singlet solution in v -space, using the non-singlet kernel $K_{ns}(v) \equiv \mathcal{L}^{-1} [e^{\tau\Phi_{ns}(s)}; v]$, by employing the Laplace convolution relation

$$F_{ns}(v, Q^2) = \int_0^v K_{ns}(v-w, \tau(Q^2, Q_0^2)) \hat{F}_{ns0}(w) dw. \quad (31)$$

For brevity, we will not pursue the case of the non-singlet solution any further here except to note that in LO, the $\Phi_{ns}(s)$ in Eq. (30) is identical to $\Phi_f(s)$ defined in Eq. (13), but will concentrate instead on the more difficult case of F_s and G .

As an example of the application of this technique, we will compare the x -space singlet distribution function $F_s(x, Q^2)$ calculated from Eq. (27) starting from the MSTW initial conditions at $Q_0^2 = 1 \text{ GeV}^2$, with the LO MSTW [3] distributions. We also will compare *separately* their $G(x, Q^2)$ with the results found from Eq. (28). We evaluate the kernels $K_{FF}(u, \tau)$, $K_{FG}(u, \tau)$ in Eq. (27) and $K_{GG}(u, \tau)$, $K_{GF}(u, \tau)$ in Eq. (28) numerically, using powerful new inverse Laplace transformation algorithms [1, 2]. In order to insure continuity across the boundaries $Q^2 = M_c^2$ and M_b^2 , we will first evolve from $Q_0^2 = 1 \text{ GeV}^2$ (the MSTW Q_0^2 value) to M_c^2 and use our evolved values of $G(x, M_c^2)$ and $F_s(x, M_c^2)$ for *new* starting values $G_0(x)$ and $F_{s0}(x)$. We will then evolve to M_b^2 , repeating the process, thus insuring continuity of G and F_s at the boundaries where n_f changes. We use the MSTW values $M_c = 1.40 \text{ GeV}$, $M_c = 4.75 \text{ GeV}$, $\alpha_s(1 \text{ GeV}^2) = 0.6818$ and $\alpha_s(M_Z^2) = 0.13939$.

In Fig. 1, we show the results—in x -space—for LO $G(x, Q^2) = xg(x, Q^2)$, for 4 values of Q^2 . The curves are the published MSTW [3] LO gluon distributions, for $Q^2 = 5, 20, 100$ and $M_Z^2 \text{ GeV}^2$, bottom to top. Since the MSTW collaboration [3] started their evolution at $Q_0^2 = 1 \text{ GeV}^2$, we used F_{s0} and G_0 constructed from their values at $Q_0^2 = 1 \text{ GeV}^2$ in Eq. (28). The dots are our results for LO $G(x, Q^2)$ from Eq. (28) (converted to x -space), using the LO MSTW values for $F_{s0}(x)$ and $G_0(x)$. The agreement, over this large span of Q^2 , is quite striking. Our numerical accuracy has been investigated and is typically better than about 1 part in 10^5 at small Bjorken- x . The most serious disagreements between our calculated G and the MSTW curves are, at $x = 10^{-5}$, 1.8% and 1.6% at $Q^2 = 100 \text{ GeV}^2$ and M_Z^2 , respectively, which is approximately within their stated numerical errors.

In Fig. 2, we show the results—in x -space—for the LO singlet distribution $F_s(x, Q^2)$, for 4 values of Q^2 , where again F_{s0} and G_0 are the MSTW [3] values at their initial evolution value of $Q_0^2 = 1 \text{ GeV}^2$. The curves are the published MSTW [3] LO singlet distributions, for $Q^2 = 5, 20, 100$ and $M_Z^2 \text{ GeV}^2$, bottom to top. The dots are our results for LO $F_s(x, Q^2)$ from Eq. (27) (converted to x -space), using the LO MSTW values for $F_{s0}(x)$ and $G_0(x)$. Again, the agreement is excellent over the entire range of Bjorken- x and virtuality Q^2 . The most serious disagreements between our calculated F_s and the MSTW curves are, at $x = 10^{-5}$, 2.0% and 1.7%, at $Q^2 = 100 \text{ GeV}^2$ and M_Z^2 , respectively. It is clear from Fig. 1 and Fig. 2 for G_s and F_s —over the enormous virtuality and x span—that our analytic solutions of Eq. (27) and Eq. (28) are correct. The numerical values were evaluated using *Mathematica* [13].

In conclusion, we have constructed *decoupled* analytical evolution equations for $F_s(x, Q^2)$ and $G(x, Q^2)$ from the coupled LO DGLAP equations. These require only a knowledge $F_{s0}(x)$ and $G_0(x)$, the initial values of F_s and G at the starting value Q_0^2 for the evolution, to calculate $F_s(x, Q^2)$ and $G(x, Q^2)$. The same procedures can be used for non-singlet distributions, allowing one to obtain *analytic* solutions for *individual* quark distributions, as well as for the gluon distribution, avoiding the necessity for numerical solutions of the coupled DGLAP on a two-dimensional grid in x, Q^2 . In essence, in a program such as *Mathematica*, we could define a function for each quark and gluon, and by inputting the desired x and Q^2 , simply evaluate it, accurately and rapidly.

We demonstrated numerically that the method gives agreement with published MSTW [3] LO values of $G(x, Q^2)$ and $F_s(x, Q^2)$ over an enormous range of x and Q^2 . The accuracy obtained using our analytic solution and fast new algorithms for performing inverse Laplace transforms [1, 2] was better than 1 part in 10^5 . In the future, as well as evaluating non-singlet distributions and the NLO singlet case, we will evaluate $F_{s0}(x)$ and $G_0(x)$ in both LO and NLO, from a fit to small x experimental data for the structure function $F_2^{\gamma p}(x, Q^2)$, in order to analytically obtain accurate values of $G(x, Q^2)$ that are *directly* tied to experiment, which are needed for the LHC.

The authors would like to thank the Aspen Center for Physics for its hospitality during the time parts of this work were done. P. Ha would like to thank Towson University Fisher College of Science and Mathematics for travel support. D.W.M. receives support from DOE Grant No. DE-FG02-04ER41308.

-
- [1] M. M. Block, Eur. Phys. J. C **65**, 1 (2010).
 - [2] M. M. Block, private communication (2010).
 - [3] A. D. Martin, W. J. Stirling, R. S. Thorne, and G. Watt, Eur. Phys. J. C **63**, 189 (2009), arXiv:0901.0002.
 - [4] V. N. Gribov and L. N. Lipatov, Sov. J. Nucl. Phys. **15**, 438 (1972).
 - [5] G. Altarelli and G. Parisi, Nucl. Phys. B **126**, 298 (1977).
 - [6] Y. L. Dokshitzer, Sov. Phys. JETP **46**, 641 (1977).
 - [7] J. Pumplin et al. (CTEQ), J. High Energy Phys. **07**, 012 (2002), hep-ph/0201195.
 - [8] W. K. Tung, H. L. Lai, A. Belyaev, J. Pumplin, D. Stump, and C.-P. Yuan, J. High Energy Phys. **02**, 053 (2007), hep-ph/0611254.
 - [9] A. D. Martin, R. G. Roberts, W. J. Stirling, and R. S. Thorne, Eur. Phys. J. C **23**, 73 (2002), hep-ph/0110215.
 - [10] A. D. Martin, R. G. Roberts, W. J. Stirling, and R. S. Thorne, Phys. Lett. B **604**, 61 (2004), hep-ph/0410230.

- [11] M. M. Block, L. Durand, and D. W. McKay, Phys. Rev. D **77**, 094003 (2008), arXiv:0710.3212 [hep-ph].
 [12] M. M. Block, L. Durand, and D. W. McKay, Phys. Rev. D **79**, 014031 (2009), arXiv:0808.0201 [hep-ph].
 [13] *Mathematica* 7, a computing program from Wolfram Research, Inc., Champaign, IL, USA, www.wolfram.com (2009).

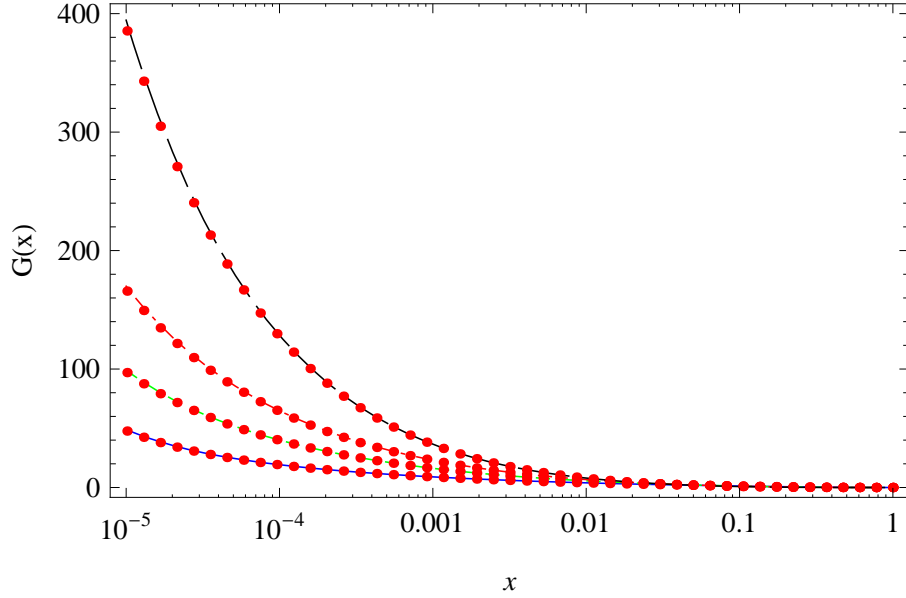


FIG. 1: The LO MSTW [3] gluon distribution, $G(x, Q^2) = xg(x, Q^2)$, for $Q^2 = 5, 20, 100$ and M_Z^2 GeV². The published MSTW [3] curves are for $Q^2 = 5, 20, 100$ and M_Z^2 GeV², bottom to top. The dots are the evolution results for LO $G(x, Q^2)$ from Eq. (28) (converted to x -space), using the LO MSTW values for $F_{s0}(x)$ and $G_0(x)$, where $Q_0^2 = 1$ GeV².

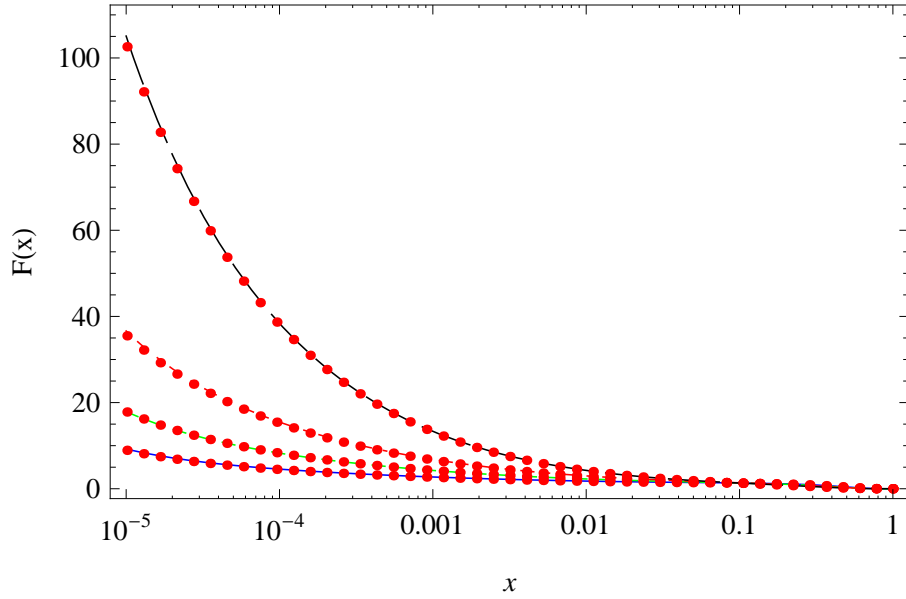


FIG. 2: The LO MSTW [3] singlet distribution, $F_s(x, Q^2)$, for $Q^2 = 5, 20, 100$ and M_Z^2 GeV². The published MSTW [3] curves are for $Q^2 = 5, 20, 100$ and M_Z^2 GeV², bottom to top. The dots are the evolution results for LO $F_s(x, Q^2)$ from Eq. (27) (converted to x -space), using the LO MSTW values for $F_{s0}(x)$ and $G_0(x)$, where $Q_0^2 = 1$ GeV².